Integrating multiple stubs in stepped-impedance filter aiming for high selectivity

Abdul Sami,[1,✉] Miguel Angel Gomez Laso,[1] Txema Lopetegi,[1] Israel Arnedo,[1] Ibai Calero,[1] Fernando Teberio,[1] Petronilo Martin Iglesias,[1,2] David Benito,[1] and Ivan Arregui[1]

[1] *Institute of Smart Cities (ISC), Department of Electrical, Electronic and Communication Engineering, Public University of Navarre (UPNA), Pamplona, Spain*

[2] *European Space Agency (ESA)-ESTEC, Noordwijk, The Netherland*

✉Email: abdul.sami@unavarra.es

A design technique to include multiple and fully-controlled transmission zeros (TZs) in the frequency response of rectangular waveguide commensurate-line stepped-impedance filters is presented in this letter. These bandpass filters (BPFs) are known for having reduced sensitivities against manufacturing inaccuracies and are composed of multiple waveguide sections. In order to improve their selectivity, $3\lambda_g/4$ and $\lambda_g/4$-stubs are included to create multiple TZs around the passband. The proposed technique allows us to add multiple stubs in a single section and, therefore, only minor adjustments in the affected part of the filter are required, which simplifies the overall design process. The technique has been verified with a design example with four TZs (two on each side) near the passband.

Introduction: High selectivity is a key factor to suppress the interferences that exist at the nearby frequencies to the passband of a filter. Different techniques are used to generate transmission zeros (TZs) near the passband to enhance this parameter, for instance the cross-couplings method [1] or the use of non-resonating modes [2]. Moreover, $\lambda_g/4$-stubs can be also used to generate TZs at specific positions to enhance selectivity as presented in [3], where $\lambda_g/4$-stubs are added to the inductively coupled classical iris bandpass filter, being λ_g the guided wavelength associated with the frequency of the TZ. However, the inclusion of multiple TZs employing these methods can lead to filters with complex geometries or devices that require long optimization processes to be designed.

Rectangular waveguide stepped-impedance filters based on commensurate lines are typically employed to obtain low-pass waveguide filters [4]. In [5, 6], the first passband replica of these structures was used to design bandpass filters (BPFs), significantly increasing the fabrication tolerances compared with the classical inductive iris filters. These BPFs are implemented with stepped-impedance waveguide sections and allow novel topologies, such as the meandered filters proposed in [7] to reduce their overall footprint. Recently, a modular design strategy to generate TZs in the stepped-impedance BPFs has been presented to improve their selectivity [8], where two $\lambda_g/4$-stubs were added to two different waveguide sections to create two TZs. In this paper, we will significantly extend this idea, proposing a technique where several stubs of different lengths will be included in the same waveguide section. Only that section would need to be re-designed for the inclusion of an arbitrary number of TZs at fully controlled positions below and above the passband while the rest of the filter can remain unaltered.

Design method: As it is detailed in [5, 6], in order to design a stepped-impedance BPF based on commensurate lines, the order of the filter N, the in-band return loss level, the type of filtering function, and the lower and upper cut-off frequencies (f_1 and f_2) of the device must be specified to calculate the impedances Z_n of the $N + 2$ commensurate lines of the prototype that satisfy the specified frequency response. Then, the characteristic impedance values are modelled with waveguide sections where both the width, a_n, and height, b_n, can be varied. Assuming TE_{10}-mode propagation, a_n and b_n are related through (1) [6]

$$b_n = Z_n \sqrt{\left(\frac{2 \times \pi \times f_\pi}{c}\right)^2 - \left(\frac{\pi}{a_n}\right)^2} \tag{1}$$

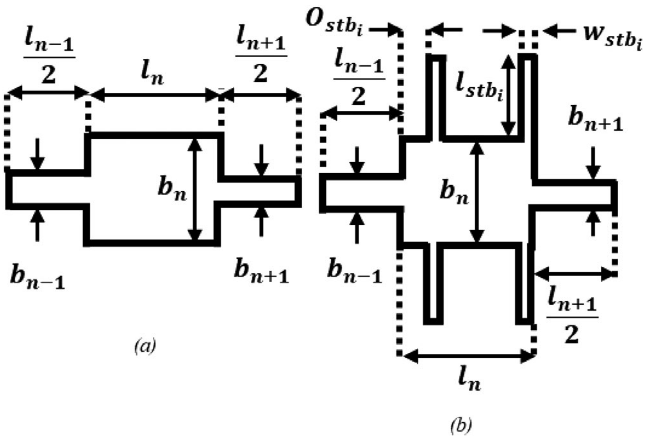

Fig. 1 *Schematic of (a) DE and (b) M-SADE (*M = *4 in this case).*

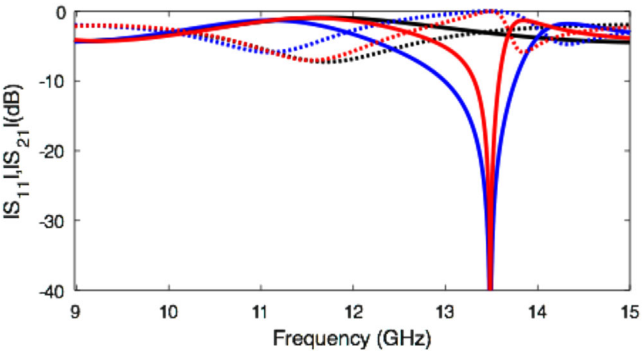

Fig. 2 *Frequency response of a DE (black line), SADE with $\lambda_g/4$-stub (blue line), and SADE with $3\lambda_g/4$-stub (red line). Dotted line: $|S_{11}|$, solid line: $|S_{21}|$.*

where c is the speed of light in vacuum and f_π is the central frequency of the passband calculated as in [7]. As the BPF is based on commensurate lines, the electrical length $\pi - \theta_c$ and $\pi + \theta_c$ of the commensurate lines correspond to f_1 and f_2, respectively, where π is the electrical length that corresponds to the middle frequency of the passband and θ_c is given by (2) [7]

$$\theta_c = \pi \times \frac{\lambda_{f1} - \lambda_{f2}}{\lambda_{f1} + \lambda_{f2}} \tag{2}$$

being λ_{fi} the wavelength related to frequency f_i. Therefore, all the waveguide sections should have the same length, l_n, ideally equal to $\lambda_\pi/2$. However, due to the discontinuities at the junctions between the different sections, these lengths must be modified to compensate for the fringing field effect. This can be done by satisfying the phase conditions for S_{11} and S_{21} given also in [7].

Once the stepped-impedance baseline filter is designed, design entities (DEs) consisting of a complete waveguide section and adjacent sections of half-length as shown in Figure 1a can be defined. This strategy was employed in [8] to modify the DE and include a $\lambda_g/4$-stub in the sections, obtaining a stub-added design entity (SADE) to create a TZ in the frequency response. However, the design technique in [8] permitted only one TZ per section and a different section had to be used per TZ. In this work, a multiple SADE (*M*-SADE) is proposed to include multiple TZs in a single section (Figure 1b), therefore simplifying the design process as the rest of the filter can be kept unaltered.

Firstly, an independent DE must be defined and simulated, obtaining a frequency response as the one shown in Figure 2 (black line). Then, any stub of length equal to odd multiples of $\lambda_g/4$ can be used to create TZs in the filter response. In Figure 2, the frequency response of a SADE with a $\lambda_g/4$-stub is also shown (blue line). As can be seen, the inclusion of a $\lambda_g/4$-stub to introduce a TZ close to the pole has shifted the pole towards lower frequencies, which will require a slight adjustment of the section length to replicate the rest of the original frequency response of the DE. It is interesting to note that when a $3\lambda_g/4$-stub is included in the

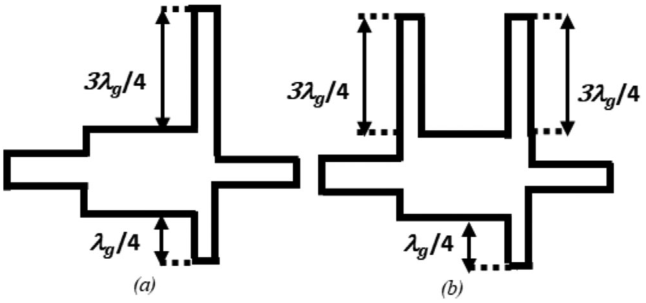

Fig. 3 *Schematic of (a) M-SADE with* M = 2 *(one* λ_g*/4-stub and one 3*λ_g*/4-stub), (b) M-SADE with* M = 3 *(one* λ_g*/4-stub and two 3*λ_g*/4-stubs).*

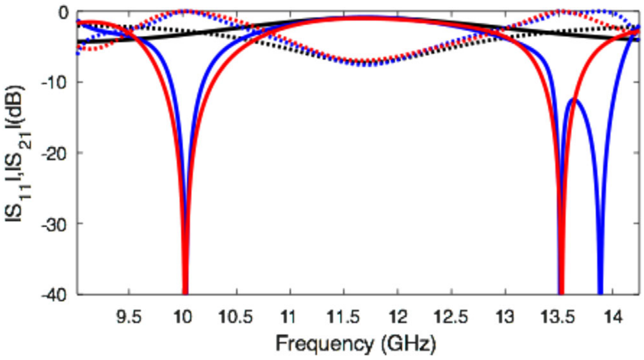

Fig. 4 *Frequency response of a DE (black line), M-SADE with* M = 2 *(red line), and M-SADE with* M = 3 *(blue line). Dotted line: |*S_{11}*|, solid line: |*S_{21}*|.*

DE, the shift of the corresponding pole is almost negligible (the red line in Figure 2), which would facilitate in some cases the design process. As explained in [3], the TZ associated with this longer stub has a narrower bandwidth compared with the TZ due to a λ_g/4-stub, which permits us to place the TZ close to the passband while barely affecting the rest of the original response. Then, the use of 3λ_g/4-stubs may be a good choice when TZs very near the passband are needed.

In general, a combination of multiple (M) λ_g/4- or 3λ_g/4-stubs can be used in the DE to design the new M-SADE depending on the frequency needs. Although it is not mandatory, the stubs should be placed at the ends of the sections since this facilitates the inclusion of multiple TZs in the frequency response without generating unwanted resonances. In Figure 3a, two stubs of lengths λ_g/4 and 3λ_g/4 are employed to create TZs at the lower and upper sides of the intrinsic pole of the DE. In order to maintain the rest of the frequency response of the baseline filter, the original frequency response of the DE must be replicated (except for the TZs, of course) by the M-SADE by adjusting b_n and l_n to fulfil (3), [8]

$$S_{11\_DE}\ (f) = S_{11_{M-SADE}}\ (f)\ \ f_1 < f < f_2 \tag{3}$$

The frequency response of the M-SADE ($M = 2$) is shown in Figure 4 (red line). Similarly, an M-SADE with $M = 3$ (Figure 3b) can be employed to include 3 TZs (2 TZs above and 1 TZ below in this case), as shown in Figure 4 (blue line). In this way, an M-SADE with multiple stubs can be designed to implement the desired combination of TZs and, afterwards, simply added to the baseline filter replacing the corresponding DE.

Design example: According to the design method explained in the last section, the first step is to design a stepped-impedance BPF based on commensurate lines. For instance, for Ku-band applications [5, 6], seventh-order ($N = 7$) Chebyshev bandpass response can be achieved between $f_1 = 10.70$ GHz and $f_2 = 12.75$ GHz with in-band return losses better than 20 dB using the following normalized impedances Z_n: $Z_0 = Z_8 = 1$, $Z_1 = Z_7 = 1.84$, $Z_2 = Z_6 = 0.40$, $Z_3 = Z_5 = 3.32$, $Z_4 = 0.32$, assuming a constant width equal to $a = 19.05$ mm and an initial height $b_0 = 3.8$ mm. Afterwards, the heights of the sections, b_n, for the corresponding Z_n are calculated using (1) and l_n is adjusted satisfying the phase conditions given in [7]. The dimensions of the filter are listed in Table 1 and the frequency response in Figure 8 (blue line).

Table 1. Dimensions of the filter structures (all parameters in mm)

Parameters	Baseline filter	Final device* *with rounded corners for fabrication
b_{t1}; l_{t1}	-	8.48; 8.71
b_{t2}; l_{t2}	-	6.42; 8.50
b_{t3}; l_{t3}	-	4.86; 5.58
b_0; l_0	3.80; 8.68	4.34; 8.68
b_1; l_1	6.99; 17.80	4.92; 23.20
b_2; l_2	1.50; 15.84	1.80; 15.23
b_3; l_3	12.62; 17.49	14.70; 17.44
b_4; l_4	1.23; 15.74	1.36; 15.53
b_5; l_5	12.62; 17.49	13.59; 17.54
b_6; l_6	1.50; 15.84	1.64; 15.79
b_7; l_7	6.99; 17.80	7.10; 17.85
b_8; l_8	3.80; 8.68	4.056; 8.68
b_{t4}; l_{t4}	-	4.59; 8.57
b_{t5}; l_{t5}	-	6.21; 8.47
b_{t6}; l_{t6}	-	8.41; 8.70
l_{stbv1}; l_{stbh1}; o_{stb1}	-	8.6; 11.15; 22.15
l_{stbv2}; l_{stbh2}; o_{stb2}	-	3.05; 8.6; 22.15
l_{stbv3}; l_{stbh3}; o_{stb3}	-	5.05; 14.15; 2.85
l_{stbv4}; l_{stbh4}; o_{stb4}	-	6.05; 7.75; 2.85

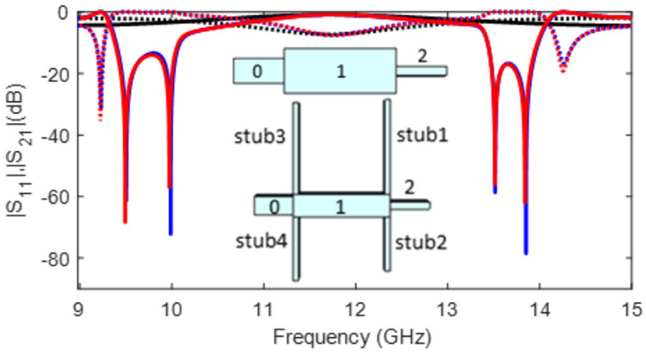

Fig. 5 *Frequency response of the DE (black line), 4-SADE with straight stubs (blue line) and 4-SADE with folded stubs used in the design example (red line). Dotted line: |*S_{11}*|, solid line: |*S_{21}*|. Inset: schematic of the* DE_1 *and the 4-SADE with straight stubs.*

Once the baseline filter has been designed for the required specifications, the next step is to design an M-SADE to create multiple TZs at the desired frequencies. A 4-SADE is designed to replace the first DE in the filter, DE_1, having four stubs which are employed to create TZs at 9.5, 10, 13.5, and 13.9 GHz. Specifically, λ_g/4-stubs are used to create TZs below the passband (9.5, 10 GHz) and 3λ_g/4-stubs are employed for the TZs above it (13.5 and 13.9 GHz). However, other combinations may be also used. In order to fulfil (3), the parameters b_1 and l_1 are slightly adjusted to replicate the frequency response of DE_1. The width of the stubs, w_{stb_i} ($w_{stb_1} = w_{stb_2} = w_{stb_3} = w_{stb_4}$), is fixed to 1.05 mm to facilitate a standard computer numerical control (CNC) milling manufacturing process. The frequency response of the DE compared with the 4-SADE is shown in Figure 5.

In order to reduce the total footprint of the device the stubs can be folded if needed, having no effect on the 4-SADE frequency response (see Figure 5). Finally, the 4-SADE is integrated in the baseline filter replacing DE_1. The resulting structure obtained is shown in Figure 6.

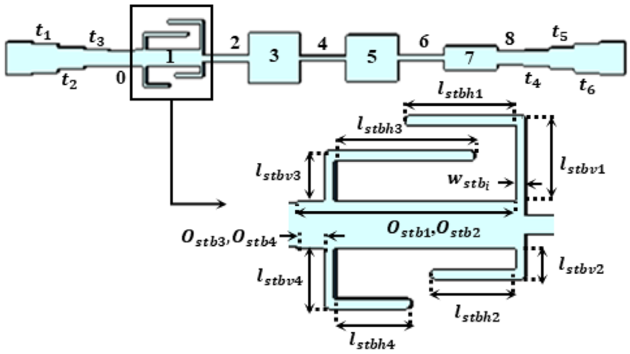

Fig. 6 *Schematic of the filter with integrated stubs.*

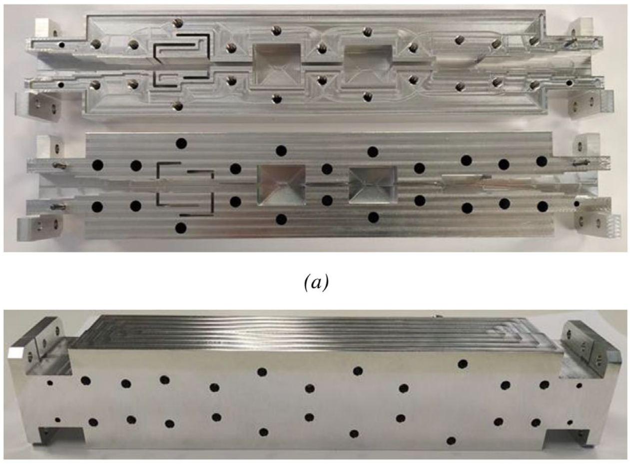

(a)

(b)

Fig. 7 *Photograph of the prototype: (a) un-assembled, (b) assembled*

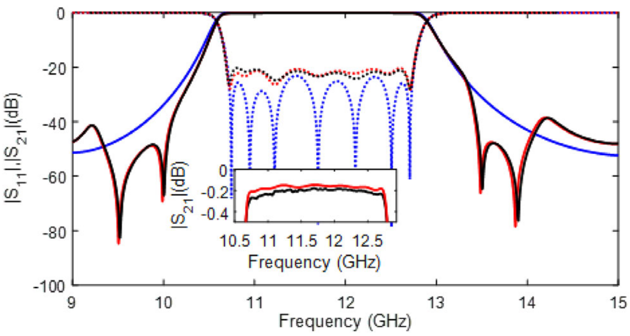

Fig. 8 *Response of the baseline filter (blue line), simulated response (red) and measured response of the proposed device (black line). $|S_{11}|$ in dotted line, $|S_{21}|$ in solid line. Inset: detail of the insertion loss*

After that, the parameters are optimized to obtain the required response to consider the effect of the rounded corners of radii equal to 0.5 mm needed to fabricate the structure using CNC milling. The final dimensions of the device are given in Table 1, including the required tapers employed to reach to the standard WR-75 waveguide ports. Each taper t_i consists of three sections with different heights, b_{ti}, and lengths, l_{ti}. The structure has been fabricated using bare aluminium in two halves (see Figure 7) along the E-plane. The simulated response (red line) is in excellent agreement with the measured frequency response (black line), as shown in Figure 8. The measured in-band return loss is better than 20 dB and the measured insertion loss is 0.22 dB at the centre frequency of the passband. The insertion loss detail is given in the inset of Figure 8.

Conclusion: A design technique to add multiple and fully controlled TZs to improve the selectivity of commensurate-line stepped-impedance BPFs has been presented. It allows us to replace one of the DEs with the proposed *M*-SADE, which permits us to include *M* TZs below or above the passband of the filter as demanded. The technique requires us to redesign one filter section only while the rest can be kept unaltered. The technique has been tested with a filter for Ku-band applications (10.7–12.75 GHz), including four TZs around the passband. The final device has been fabricated by CNC milling in aluminium, confirming the simulated frequency response. Therefore, the proposed technique can be considered an interesting alternative to design BPFs with a wide passband and TZs below and above this passband.

Acknowledgements: This work was supported by the Spanish Ministerio de Ciencia e Innovación –Agencia Estatal de Investigación (MCIN/AEI/10.13039/501100011033) under Project PID2020-112545RB-C53 and by the European Union's Horizon 2020 Research and Innovation Program under Grant 811232-TESLA-H2020-MSCA-ITN-2018.

Conflict of interest: The authors declare no conflict of interest.

Data availability statement: Data sharing not applicable to this article as no datasets were generated or analyzed during the current study.

© 2022 The Authors. *Electronics Letters* published by John Wiley & Sons Ltd on behalf of The Institution of Engineering and Technology.

This is an open access article under the terms of the Creative Commons Attribution License, which permits use, distribution and reproduction in any medium, provided the original work is properly cited.
Received: *10 March 2022* Accepted: *27 April 2022*
doi: 10.1049/ell2.12517

References

1 Shen, T., Zaki, K.A., Atia, A.E.: Full-wave design of canonical waveguide filters by optimization. *IEEE MTT-S Int. Microw. Symp. Dig.* **3**, 1487–1490 (2001)
2 Bastioli, S., Tomassoni, C., Sorrentino, R. A.: New class of waveguide dual-mode filters using TM and non-resonating modes. *IEEE Trans. Microw. Theory Tech.* **58**(12), 3909–3917 (2010)
3 Carceller, C., Soto, P., Boria, V., Guglielmi, M.: Capacitive obstacle realizing multiple transmission zeros for in-line rectangular waveguide filters. *Microwave Wirel. Components Lett.* **26**(10), 795–797 (2016)
4 Cameron, R.J., Kudsia, C.M., Mansour, R.R.: *Microwave Filters for Communication Systems: Fundamentals*. John Wiley & Sons, New York 2018
5 Teberio, F., Soto, P., Arregui, I., Lopetegi, T., Cogollos, S., Arnedo, I., Martin-Iglesias, P., Boria, V.E., Laso, M.A.: Waveguide band-pass filter with reduced sensitivity to fabrication tolerances for Q-band payloads. In: IEEE MTT-S International Microwave Symposium (IMS), pp. 1464–1467 (2017)
6 Sami, A., Teberio, F., Miranda, L., Arnedo, I., Martin-Iglesias, P., Benito, D., Lopetegi, T., Laso, M.A., Arregui, I.: Robust tolerance design of bandpass filter with improved frequency response for Q-band satellite applications. *IEEE Microw. Wirel. Components Lett.* **31**(11), 1183–1186 (2021)
7 Teberio, F., Percaz, J.M., Arregui, I., Martin-Iglesias, P., Lopetegi, T., Laso, M.A., Arnedo, I.: Rectangular waveguide filters with meandered topology. *IEEE Trans. Microw. Theory Tech.* **66**(8), 3632–3643 (2018)
8 Miranda, L. Teberio, F., Martin-Iglesias, P., Calero, I., Arregui, I., Arnedo, I., Percaz, J.M., Santiago, D., Lopetegi, T., Laso, M.A.: Stepped-impedance band-pass filters with improved selectivity. In: IEEE MTT-S International Microwave Symposium (IMS), pp. 1198–1200 (2019)